A *triskelion*-shaped saddle-helix hybrid nanographene

Carlos M. Cruz,[a] Irene R. Márquez,[a] Silvia Castro-Fernández,[a] Juan M. Cuerva,[a] Ermelinda Maçôas,[b] and Araceli G. Campaña*[a]

Abstract: A unique rippled nanographene constituted by 52 fused rings is presented in which six out-of-plane motifs are fully fused into a triangular aromatic surface of *ca.* 2.5 nm size. Three units of an unprecedented fully lateral π-extended octabenzo[5]helicene together with three units of saddle-shaped heptagonal rings are combined in a single structure leading to a well-soluble warped nanographene. The two pairs of possible enantiomers have been isolated and their linear, non-linear and chiroptical properties evaluated, revealing an outstanding quantum yield and brightness values at low energy together with good chiroptical responses both in the absorption and emission.

The well-defined bottom-up synthesis of nonplanar polycyclic aromatic hydrocarbons (PAHs) is receiving increasing attention in order to incorporate new physical properties to their flat counterparts.[1] Besides bowls, hoops or twisted acenes,[2] saddle-shaped[3] together with helical aromatics[4] constitute two important classes of non-planar carbon based π-conjugated systems. Both fields are developing promptly due to they offer unique properties, such as low molecular aggregation, high solubility and dynamic behavior, to the final compounds. Furthermore, negatively curved saddle aromatics, generally caused by the inclusion of a heptagon or octagon, have been proposed to show interesting mechanical, electronic and magnetic properties[5] while non-racemizable enantiopure carbo[n]helicene systems are characterized by their intrinsic chiroptical properties, such as optical rotation, circular dichroism,[6] or chiral-induced spin selectivity (CISS) effect[7] finding applications as switches or sensors.[4a]

Combining both curved motifs, namely a seven-membered carbocycle and a carbo[n]helicene in a single conjugated structure would lead to exotic distorted geometries and, more importantly, novel synergy of interesting properties. Despite its potentiality, saddle-helix hybrid compounds are very scarce.[8] However, we have recently demonstrated[9] that the concurrent inclusion of both non-planar motifs into nanographene ribbons leads to new combination of optical properties in graphene-related materials, namely upconversion based on two-photon absorption (TPA-UC) together with circularly polarized luminescence (CPL).[10] Simultaneously, unique structural motifs, such as laterally π-extended pentabenzo[5]helicene[9a] or heptabenzo[7]helicene[9b] units, were created in such distorted PAHs. Those enantiopure helix led to the first CPL-active

nanographenes, opening the door to new optoelectronic applications for carbon nanomaterials.[11]

In our search for new curved aromatics with novel physical properties, we realized that saddle-helix hybrid compounds are limited either to relatively small size[8] (up to 17 conjugated aromatic rings) or ribbon-shaped PAHs[9] with only three examples reported of enantiopure saddle-helix hybrid compounds (Fig. 1).[8d],[9] However, larger π-conjugated PAHs (extended over 1 nm) have demonstrated improved properties in terms of defined low band gaps depending on their sizes and edges, with potential applications in nano and optoelectronics.[12] Therefore, we were motivated to present a synthetic large nanographene incorporating multiple saddle and enantiopure helix curvatures leading to a novel well-defined π-extended warped nanographene and evaluate its photophysical properties. In this sense, in recent years it has been shown that multiple and laterally π-extended carbo[n]helicenes own interesting properties and applications that would not be accessible to single helicenes.[13] On the other hand, the simultaneous inclusion of several heptagons in a single PAH has led to highly warped carbon nanostructures of increasing complexity.[8c],[9b],[14] It is expected that the incorporation of several units of each curved motif into a large PAH would create a highly contorted aromatic structure, with modified optoelectronic properties and enhanced solubility in comparison with purely hexagonal PAHs of similar size and shape.
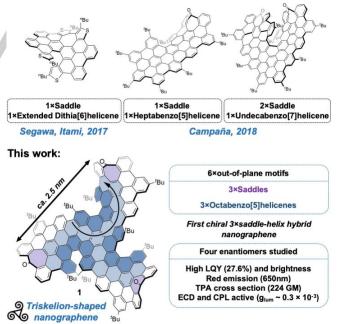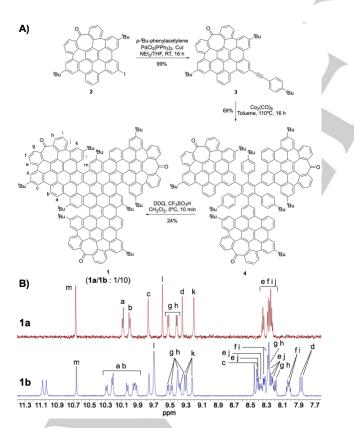
Enantiopure saddle-helix hybrid nanographenes

Figure 1. Background and novel structural features of nanographene **1**. (Enantiomer (*M,M,M*)-**1** is presented)

[a]   C. M. Cruz, Dr. I. R. Márquez, Dr. S. Castro-Fernández, Prof. J. M. Cuerva, Dr. A. G. Campaña
      Departamento de Química Orgánica, Facultad de Ciencias
      Unidad de Excelencia Química Aplicada a Biomedicina y Medioambiente. Universidad de Granada. Avda. Fuentenueva, s/n, E-18071 Granada, Spain. E-mail: araceligc@ugr.es
[b]   Dr. E. Maçôas
      Centro de Química Estructural and Institute of Nanoscience and Nanotechnology (IN), Instituto Superior Técnico.University of Lisbon Av. Rovisco Pais, 1, 1049-001 Lisboa, Portugal

      Supporting information for this article is given via a link at the end of the document.

In this work we present the synthesis, characterization and linear, non-linear and chiroptical properties evaluation of a triskelion-shaped nanographene **1** (Fig.1) as the first nanographene of significant size, over 1 nm, (153 conjugated carbon atoms and 52 fused rings) containing simultaneously three units of two curved motifs,

namely three saddle-shaped heptagonal carbocycles and three enantiopure carbo[5]helicenes. For the first time, the three helix are fully fused with the polyaromatic surface leading to a nanographene containing three unprecedented octabenzocarbo[5]helicenes. The lateral π-extension provides extra modification of the optoelectronic properties in comparison with simple helicenes as basic models for Riemann surfaces.[15] The three helix arranged in a triskelion shape generated two pairs of possible enantiomers that are characterized separately. The original incorporation of six units of out-of-plane curvatures create a unique 3D-distorted rippled nanographene **1**.

The synthesis of **1** (Scheme 1) started with our described methodology[16] for the preparation of distorted HBC analogue (hept-HBC) **2** bearing an aryl iodide for the subsequent Sonogashira cross-coupling reaction to give **3**. Following the synthetic strategy developed by Müllen to prepare PAH structures,[17] we linked three units of **3** via Co$_2$(CO)$_8$-mediated alkyne cyclotrimerization reaction generating a branched oligophenylene **4** as 1,3,5- substituted regioisomer. Still, we obtained a mixture of atropisomers (see SI, Fig. S32) that was subjected to a final Scholl-type oxidative cyclodehydrogenation to create the central HBC unit leading to nanographene **1**.

The incorporation of bulky ^{t}Bu substituents implies that three carbo[5]helicene moieties are created in this final step and therefore **1** was obtained as a mixture of the two possible diastereoisomers, C_3 symmetric (*P,P,P/M,M,M*)-**1** (**1a**) and C_1 asymmetric (*P,P,M/M,M,P*)-**1** (**1b**) pairs. Remarkably, each [5]helicene is fully lateral π-extended, constituting the first examples reported of a octabenzo[5]helicene moiety. The good solubility of **1** in organic solvents allowed its characterization by ^{1}H-NMR spectroscopy where two set of signals in a 1 to 10 ratio can be discriminated (Fig. S5).[18] High-resolution mass spectrometry (MALDI-TOF) also confirmed the isolation of **1** (C$_{189}$H$_{120}$O$_3$, [M$^+$] = 2436.9218). Subsequently, we separated both diastereoisomers of **1** by HPLC (see SI, Fig. S17). ^{1}H-NMR spectrum (Scheme 1B) of the minor compound shows only three different signals corresponding to non-equivalent ^{t}Bu groups and thirteen aromatic protons, which is in agreement with the structure of (*P,P,P/M,M,M*) pair **1a**. Major compound could then be attributed to the (*P,P,M/M,M,P*) pair **1b** as derived from its ^{1}H-NMR analysis.

Theoretically optimized structures (DFT-CAMB3LYP/6-31G (d, p)) show compound **1a** as a warped distorted C_3-symmetry nanographene of 2.46 nm side-length, centered on a planar [6]circulene fused with three distorted hept-HBCs at the edges (Fig. 2, left). The three octabenzo[5]helicene moieties show mean dihedral angles of 26.3° for **1a**, slightly higher than the one reported for a single carbo[5]helicene.[19] (For more details, see Fig. S33-34). The theoretical relative stability of both diastereoisomers was opposite to the experimentally observed 1/10 ratio of **1a**/**1b** suggesting **1a** to be slightly more stable than **1b** (ΔG(**1b-1a**) ~ 9.0 Kcal mol^{-1}). On the other side, study of **4** atropisomers shows inverse theoretical relative energies compared with those of the final products, being **4b** more stable than **4a** (ΔG(**4b-4a**) ~ −2.5 Kcal mol^{-1}, see SI, Table S1), suggesting that each diastereoisomer of **1** to come from the corresponding atropisomer of **4**.[20]

A)

B)

Scheme 1 A) Synthesis of compound **1**. **B)** Stackplot of partial ^{1}H-NMR spectra of each diastereoisomer (500 MHz, C$_2$D$_2$Cl$_4$, 293 K).
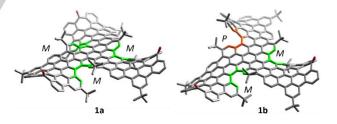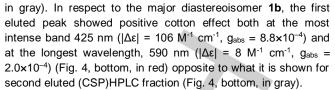

Figure 2. DFT (CAMB3LYP/6-31G (d, p)) optimized structures of **1a** and **1b** with the torsion angles of the [5]helicenes highlighted.

After comparison with other reported purely hexagonal PAHs of similar shape (triangular) and size (*ca.* 2.5 nm side) that present very poor solubility even with the presence of side alkyl chains,[21] it is clear that, in the case of **1**, it is the great curvature what increased solubility, thus allowing a rigorous evaluation of photophysical properties. Both compounds **1a**/**1b** presented magenta color when dissolved in CH$_2$Cl$_2$. Their UV-Vis absorption spectra (Fig. 3) showed a vibronic structure with high molar absorptivity coefficients at the maximum absortion bands, at 517/522 nm (ε = 2.97/4.12 × 10^5 M^{-1} cm^{-1}) for **1a**/**1b**,

respectively. Remarkably, this last value is one order of magnitude higher than common dyes such as perilene diimides (PDI)[22] and represent a 4-fold and 2.7-fold increase in comparison with multiple-PDI based nanoribbons and nanographenes, respectively.[6],[23]

The fluorescence spectra of both diastereoisomers (Fig. 3) showed an intense red emission centered at 643/650 nm for **1a/1b**, respectively, extending to 750 nm with high luminescence quantum yield (LQY) of 27.6%. This LQY is remarkably higher than that described for simple [5]helicene (4%),[24] triple dibenzo[5]helicene (2.6%),[14d] or even generally used luminescent graphene quantum dots (GQDs, usually range ~2-23%).[25] The emission lifetime is multiexponential with average values in the range of 5-6 ns (see SI, Fig S26). The optical HOMO-LUMO gaps resulted 2.01/2.06 eV for **1a/1b**, respectively). Regarding to the nonlinear optical properties, the two-photon absorption (TPA) cross-section (σ_2) of **1a** presents a value of 146 GM while **1b** presents higher σ_2 of 224 GM at *ca.* 860 nm in agreement with the observed one photon absorption. Excitation with two photons in the near infrared (750-920 nm) results in up-converted emission overlapping the one-photon-induced emission spectrum (see SI, Fig. S27). The σ_2 is in the range of previously reported ribbon-shaped nanographene or carbon nanodots.[26] Remarkably, two-photon brightness (σ_2 x LQY) is 40 GM and 62 GM for **1a** and **1b**, respectively.

Subsequently, each racemic diastereoisomer **1a/1b** was resolved into their enantiomers by chiral stationary phase (CSP)HPLC (see SI for details)[20] and their ECD spectra measured in CH_2Cl_2 showed a clear mirror image with several Cotton effects along the UV-visible range (Fig. 4).

Figure 3. UV-vis absorption (–) and normalized fluorescence (---) spectra of **1a** and **1b** in CH_2Cl_2 at *ca.* 10^{-6} M.

For symmetric **1a**, the first eluted fraction presented a positive Cotton effect at 446 nm ($|\Delta\varepsilon|$ = 252 M^{-1} cm^{-1}, g_{abs} = 8.2×10^{-3}) and two consecutive negative Cotton effect at the longest wavelengths above 500 nm that correspond to the main maximum absorption bands at the UV-vis spectrum 517 ($|\Delta\varepsilon|$ = 103 M^{-1} cm^{-1}, g_{abs} = 3.5×10^{-4}) and 550 nm ($|\Delta\varepsilon|$ = 58 M^{-1} cm^{-1}, g_{abs} = 2.5×10^{-4}) (Fig. 4, top, in red). The second eluted enantiomer exhibited the corresponding mirror image (Fig. 4, top,

in gray). In respect to the major diastereoisomer **1b**, the first eluted peak showed positive cotton effect both at the most intense band 425 nm ($|\Delta\varepsilon|$ = 106 M^{-1} cm^{-1}, g_{abs} = 8.8×10^{-4}) and at the longest wavelength, 590 nm ($|\Delta\varepsilon|$ = 8 M^{-1} cm^{-1}, g_{abs} = 2.0×10^{-4}) (Fig. 4, bottom, in red) opposite to what it is shown for second eluted (CSP)HPLC fraction (Fig. 4, bottom, in gray).

From those results, it is clearly shown that the enantiomeric forms of C_3 symmetric **1a** present considerable higher chiroptical responses in terms of the dissymmetry factor (g_{abs}) corresponding to C_1 asymmetric **1b**. The assignment of each of the four enantiomers chirality was done by comparison of the experimental ECD with the TD-DFT simulated ECD spectra (see SI, Fig. S36-S38). Thus, the first (CSP)HPLC fractions correspond with (*P,P,P*)-**1a** and (*M,M,P*)-**1b** enantiomers, respectively.

Finally, as expected from a chiral and emissive compound, **1** resulted active in CPL, becoming part of the still exclusive family of CPL emissive nanographenes.[9] Thus, the CPL of the four enantiomers was measured and the enantiomeric forms of each **1a** and **1b** gave CPL of opposite signs as expected for pure CPL (Fig. 4).[27] Likewise, the sign of the CPL spectra are in both cases in good correlation with the sign of the longest wavelength ECD band. Regarding **1a** (Fig. 4, top, in wine and black), the CPL spectra of both enantiomers show a maximum centered at 643 nm with a similar profile to the corresponding fluorescence spectrum and a g_{lum} value estimated as 3 × 10^{-4}. In the case of the enantiomeric forms of **1b**, the CPL maximum is centered at 656 nm (Fig. 4, bottom in wine and black) with a g_{lum} value of 2 × 10^{-4}.
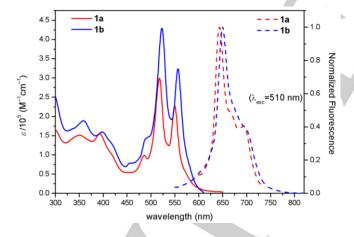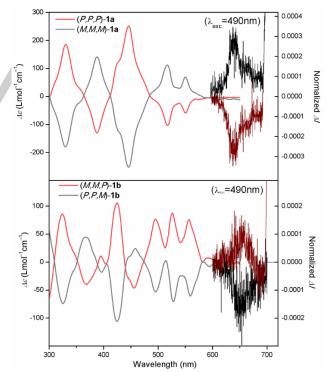

Figure 4. Experimental ECD (300-600 nm) and CPL (600-700 nm) of **1a** and **1b** enantiomers in CH_2Cl_2 at *ca.* 2-5×10^{-6} M.

The synthesis of **1** constitutes a novel example of strategic combination of curved structural motifs into a single PAH, leading to a large and well-defined rippled nanographene. We created a unique triskelion-shaped PAH in which three units of two curved motifs are fully fused with the extended aromatic surface. The first lateral π-extended octabenzo[5]helicene unit is presented, and remarkably three units of this moiety are embedded into a single nanographene and their distinctive triangular disposition affords two pairs of enantiomeric forms that have been isolated. Their linear, non-linear and chiroptical properties have been studied, revealing outstanding quantum yield and brightness values at low energy joined to good ECD and CPL responses. As suggested recently, the inclusion of curvatures in PAHs plays a key role improving their planar equivalents as emitters in OLEDs.[28] Our work contributes to the understanding of the structure-properties relationship in carbon nanostructures encouraging to the next step of the bespoke design of saddle-helix hybrid graphene molecules.

Acknowledgements

Keywords: nanographenes • helicenes • circularly polarized luminescence • nanostructures • nonlinear optics

[1] a) A. Hashimoto, K. Suenaga, A. Gloxer, K. Urita, S. Iijima, *Nature* **2004**, *430*, 867-870; b) K. K. Baldridge, J. S. Siegel, *Angew. Chem. Int. Ed.* **2013**, *52*, 5436-5438; c) S. T. Skowron, I. V. Lebedeva, A. M. Popov, E. Bichoutskaia, *Chem. Soc. Rev.* **2015**, *44*, 3143-3176; d) Y. Segawa, H. Ito, K. Itami, *Nat. Rev. Mat.* **2016**, *1*, 1-14.

[2] a) Y.-T. Wu, J. S. Siegel, *Chem. Rev.* **2006**, *106*, 4843-4867; b) R. A. Pascal Jr., *Chem. Rev.*, **2006**, *106*, 4809–4819; c) M. A. Majewski, M. Stepien, *Angew. Chem. Int. Ed.* **2019**, *58*, 86-116; *Angew. Chem.* **2019**, *131*, 90-122; d) Y. Xiao, J. T. Mague, R. H. Schmehl, F. M. Haque, R. A. Pascal Jr., *Angew. Chem. Int. Ed.* **2019**, *58*, 2831-2833. Selected examples of bowl-graphene and bowl-helix hybrids: e) A. K. Dutta, A. Linden, L. Zoppi, K. K. Baldridge, J. S. Siegel, *Angew. Chem. Int. Ed.* **2015**, *54*, 10792-10796; f) D. Meng, G. Liu, C. Xiao, Y. Shi, L. Zhang, L. Jiang, K. K. Baldridge, Y. Li, J. S. Siegel, Z. Wang, *J. Am. Chem. Soc.* **2019**, DOI: 10.1021/jacs.9b00053.

[3] a) I. R. Márquez, S. Castro-Fernández, A. Millán, A. G. Campaña, *Chem. Commun.* **2018**, *54*, 6705-6718; b) S. H. Pun, Q. Miao, *Acc. Chem. Res.* **2018**, *51*, 1630-1642.

[4] a) Y. Shen, C. F. Chen, *Chem. Rev.* **2012**, *112*, 1463-1535; b) M. Gingras, *Chem. Soc. Rev.* **2013**, *42*, 968-1006; c) M. Rickhaus, M. Mayor, M. Juríček, *Chem. Soc. Rev.* **2016**, *45*, 1542-1556; d) D. Reger, P. Haines, F. W. Heinemann, D. M. Guldi, N. Jux, *Angew. Chem. Int. Ed.* **2018**, *57*, 5938-5942; *Angew. Chem.* **2018**, *130*, 6044-6049; e) P. J. Evans, J. Ouyang, L. Favereau, J. Crassous, I. Fernández, J. Perles, N. Martín, *Angew. Chem. Int. Ed.* **2018**, *57*, 6774-6779; *Angew. Chem.* **2018**, *130*, 6890-6895.

[5] a) T. Lenosky, X. Gonze, M. Teter, V. Elser, *Nature* **1992**, *355*, 333-335; b) N. Park, M. Yoon, S. Berber, J. Ihm, E. Osawa, D. Tománek, *Phys. Rev. Lett.* **2003**, *91*, 237204; c) D. Odkhuu, D. H. Jung, H. Lee, S. S. Han, S.-H. Choi, R. S. Ruoff, N. Park, *Carbon* **2014**, *66*, 39-47.

[6] N. J. Schuster, R. H. Sánchez, D. Bukharina, N. A. Kotov, N. Berova, F. Ng, M. L. Steigerwald, C. Nuckolls, *J. Am. Chem. Soc.* **2018**, *140*, 6235-6239.

[7] V. Kiran, S. P. Mathew, S. R. Cohen, I. H. Delgado, J. Lacour, R. Naaman, *Adv. Mater.* **2016**, *28*, 1957-1962.

[8] a) J. Luo, X. Xu, R. Mao, Q. Miao, *J. Am. Chem. Soc.* **2012**, *134*, 13796-13803; b) A. Pradhan, P. Dechambenoit, H. Bock, F. Durola, *J. Org. Chem.* **2013**, *78*, 2266-2274; c) T. Fujikawa, Y. Segawa, K. Itami, *J. Org. Chem.* **2017**, *82*, 7745-7749; d) K. Kawai, K. Kato, L. Peng, Y. Segawa, L. T. Scott, K. Itami, *Org. Lett.* **2018**, *20*, 1932-1935.

[9] a) C. M. Cruz, I. R. Márquez, I. F. A. Mariz, V. Blanco, C. Sánchez-Sánchez, J. M. Sobrado, J. A. Martín-Gago, J. M. Cuerva, E. Maçôas, A. G. Campaña, *Chem. Sci.* **2018**, *9*, 3917-3924; b) C. M. Cruz, S. Castro-Fernández, E. Maçôas, J. M. Cuerva, A. G. Campaña, *Angew. Chem. Int. Ed.* **2018**, *57*, 14782-14786; *Angew. Chem.* **2018**, *130*, 14998-15002.

[10] a) F. Zinna, L. Di Bari, *Chirality* **2015**, *27*, 1-13; b) E. M. Sánchez-Carnerero, A. R. Agarrabeitia, F. Moreno, B. L. Maroto, G. Muller, M. J. Ortiz, S. de la Moya, *Chem. Eur. J.* **2015**, *21*, 13488-13500; c) J. Kumar, T. Nakashima, T. Kawai, *J. Phys. Chem. Lett.* **2015**, *6*, 3445-3452; d) G. Longhi, E. Castiglioni, J. Koshoubu, G. Mazzeo, S. Abbate, *Chirality* **2016**, *28*, 696-707; d) J. OuYang, J. Crassous, *Coord. Chem. Rev.* **2018**, *376*, 533-547.

[11] Y. Yang, R. C. da Costa, M. J. Fuchter, A. J. Campbell, *Nat. Photonics* **2013**, *7*, 634-638.

[12] a) J. Wu, W. Pisula, K. Müllen, *Chem. Rev.* **2007**, *107*, 718-747; b) L. Zhi, K. Müllen, *J. Mater. Chem.* **2008**, *18*, 1472-1484; c) X. Feng, W. Pisula, K. Müllen, *Pure Appl. Chem.* **2009**, *81*, 2203-2224.

[13] a) M. Rickhaus, M. Mayor, M. Juríček, *Chem. Soc. Rev.* **2017**, *46*, 1643-1660; b) C. Li, Y. Yang, Q. Miao, *Chem. Asian J.* **2018**, *13*, 884-894. Selected enantiopure multiple carbo[5]helicenes: (c) D. Peña, A. Cobas, D. Pérez, E. Guitián, L. Castedo, *Org. Lett.* **2000**, *2*, 1629-1632; (d) A. Pradhan, P. Dechambenoit, H. Bock, F. Durola, *Angew. Chem. Int. Ed.*, **2011**, *50*, 12582-12585; (e) H. Saito, A. Uchida, S. Watanabe, *J. Org. Chem.* **2017**, *82*, 5663-5668; (f) T. Hosokawa, Y. Takahashi, T. Matsushima, S. Watanabe, S. Kikkawa, I. Azumaya, A. Tsurusaki, K. Kamikawa, *J. Am. Chem. Soc.* **2017**, *139*, 18512-18521; (g) V. Berezhnaia, M. Roy, N. Vanthuyne, M. Villa, J. V. Naubron, J.-V. Rodriguez, Y. Coquerel, M. Gingras, *J. Am. Chem. Soc.* **2017**, *139*, 18508-18511. Selected enantiopure laterally π-extended carbo[5]helicenes: (h) C. L. Eversloh, Z. Liu, B. Müller, M. Stangl, C. Li, K. Müllen, *Org. Lett.* **2011**, *13*, 5528-5531; (i) S. Xiao, S. J. Kang, Y. Wu, S. Ahn, J. B. Kim, Y.-L. Loo, T. Siegrist, M. L. Steigerwald, H. Li, C. Nuckolls, *Chem. Sci.*, **2013**, *4*, 2018

[14] a) K. Kawasumi, Q. Zhang, Y. Segawa, L. T. Scott, K. Itami, *Nat. Chem.* **2013**, *5*, 739-744; b) K. Y. Cheung, X. Xu, Q. Miao, *J. Am. Chem. Soc.* **2015**, *137*, 3910-3914; c) W. S. Wong, C. F. Ng, D. Kuck, H. F. Chow, *Angew. Chem. Int. Ed.* **2017**, *56*, 12356-12360; *Angew. Chem.* **2017**, *129*, 12528-12532; d) H.-A. Lin, K. Kato, Y. Segawa, L. T. Scott, K. Itami, *Chem. Sci.* **2019**, *10*, 2326-2330.

[15] F. Xu, H. Yu, A. Sadrzadeh, B. I. Yakobson, *Nano Lett.* **2016**, *16*, 34-39.

[16] I. R. Márquez, N. Fuentes, C. M. Cruz, V. Puente-Muñoz, L. Sotorrios, M. L. Marcos, D. Choquesillo-Lazarte, B. Biel, L. Crovetto, E. Gómez-Bengoa, M. T. González, R. Martin, J. M. Cuerva, A. G. Campaña, *Chem. Sci.* **2017**, *8*, 1068-1074.

[17] P. Herwig, C. W. Kayser, K. Müllen, H. W. Spiess, *Adv. Mat.* **1996**, *8*, 510-513.

[18] Unfortunately, this high solubility handicapped the formation of single crystals for X-ray diffraction.

[19] a) R. Kuroda, *J. Chem. Soc., Perkin Trans. 2* **1982**, *7*; b) C. F. Chen, C. Y. Shen, *Helicene Chemistry, From Synthesis to Applications*, Springer, Berlin, **2017**, 19-40.

[20] Epimerization/racemization was not observed after heating a tetrachloroethane solution of **1b** at 100°C for 24 h. Additional heating led to new extra HPLC broad peaks appearing from 140°C, probably corresponding to decomposition products, thus preventing an evaluation of the epimerization barrier.

[21] a) V. S. Iyer, M. Wehmeier, J. D. Brand, M. A. Keegstra, K. Müllen, *Angew. Chem. Int. Ed.* **1997**, *36*, 1603-1607; b) J. Wu, Ž. Tomović, V. Enkelmann, K. Müllen, *J. Org. Chem.* **2004**, *69*, 5179-5186; c) X. Yan, X. Cui, B. Li, L.-s. Li, *Nano Lett.* **2010**, *10*, 1869-1873.

[22] F. Würthner, *Chem. Commun.* **2004**, 1564-1579.

[23] G. Liu, T. Koch, Y. Li, N. L. Doltsinis, Z. Wang, *Angew. Chem. Int. Ed.* **2019**, *58*, 178-183; *Angew. Chem.* **2019**, *131*, 184-189.

[24] (a) J. B. Birks, D. J. S. Birch, E. Cordemans, E. V. Donckt, *Chem. Phys. Lett.* **1976**, *43*, 33-36; (b) H. Kubo, T. Hirose, K. Matsuda, *Org. Lett.* **2017**, *19*, 1776-1779.

[25] (a) L. Li, G. Wu, G. Yang, J. Peng, J. Zhao, J. J. Zhu, *Nanoscale* **2013**, *5*, 4015-4039; (b) P. Tian, L. Tang, K. S. Teng, S. P. Lau, *Materials Today Chemistry* **2018**, *10*, 221-258.

[26] C. I. M. Santos, I. F. A. Mariz, S. N. Pinto, G. Gonçalves, I. Bdikin, P. A. A. P. Marques, M. G. P. M. S. Neves, J. M. G. Martinho, E. M. S. Maçôas, *Nanoscale* **2018**, *10*, 12505-12514.

[27] J. P. Riehl, F. S. Richardson, *Chem. Rev.* **1986**, *86*, 1-16.

[28] J. Vollbrecht, C. Wiebeler, H. Bock, S. Schumacher, H.-S. Kitzerow, *J. Phys. Chem. C.* **2019**, *123*, 4483-4492.

Entry for the Table of Contents

COMMUNICATION

Rippling the surface: a quiral nanographene constituted by four fused hexabenzocoronene-based units is presented. Six curved units are introduced into a triangular aromatic surface leading to three octabenzo[5]helicenes and three saddle edges. The two pairs of enantiomers exhibit remarkable red emission and chiroptical properties

TRISKELION-SHAPED SADDLE HELIX HYBRID NANOGRAPHENE

3 Helicenes
+
3 Heptagons

4 Enantiomers Characterized

C. M. Cruz, I. R. Márquez, S. Castro-Fernández, J. M. Cuerva, E. Maçôas, A. G. Campaña*

1 – 5

A *triskelion*-shaped saddle-helix hybrid nanographene